JGR Biogeosciences

RESEARCH ARTICLE
10.1029/2019JG005270

From Andes to Amazon: Assessing Branched Tetraether Lipids as Tracers for Soil Organic Carbon in the Madre de Dios River System

Frédérique M. S. A. Kirkels[1], Camilo Ponton[2,3], Valier Galy[4], A. Joshua West[2], Sarah J. Feakins[2], and Francien Peterse[1]

[1]Department of Earth Sciences, Utrecht University, Utrecht, The Netherlands, [2]Department of Earth Sciences, University of Southern California, Los Angeles, CA, USA, [3]Geology Department, Western Washington University, Bellingham, WA, USA, [4]Woods Hole Oceanographic Institution, Woods Hole, MA, USA

Abstract We investigate the implications of upstream processes and hydrological seasonality on the transfer of soil organic carbon (OC) from the Andes mountains to the Amazon lowlands by the Madre de Dios River (Peru), using branched glycerol dialkyl glycerol tetraether (brGDGT) lipids. The brGDGT signal in Andean soils (0.5 to 3.5 km elevation) reflects air temperature, with a lapse rate of −6.0 °C/km elevation ($r^2 = 0.89$, $p < 0.001$) and −5.6 °C/km elevation ($r^2 = 0.89$, $p < 0.001$) for organic and mineral horizons, respectively. The same compounds are present in river suspended particulate matter (SPM) with a lapse rate of −4.1 °C/km elevation ($r^2 = 0.82$, $p < 0.001$) during the wet season, where the offset in intercept between the temperature lapse rates for soils and SPM indicates upstream sourcing of brGDGTs. The lapse rate for SPM appears insensitive to an increasing relative contribution of 6-methyl isomer brGDGTs produced within the river. River depth profiles show that brGDGTs are well mixed in the river and are not affected by hydrodynamic sorting. The brGDGTs accumulate relative to OC downstream, likely due to the transition of particulate OC to the dissolved phase and input of weathered soils toward the lowlands. The temperature-altitude correlation of brGDGTs in Madre de Dios SPM contrasts with the Lower Amazon River, where the initial soil signature is altered by changes in seasonal in-river production and variable provenance of brGDGTs. Our study indicates that brGDGTs in the Madre de Dios River system are initially soil derived and highlights their use to study OC sourcing in mountainous river systems.

Plain Language Summary Rivers transport large amounts of carbon from soils to the ocean. However, following the route of carbon from mountains to river to sea is challenging in part due to the reactive nature of organic molecules in the environment. In this paper, we investigated the Madre de Dios (Peru), an upstream branch of the Amazon River, and identified carbon sources using temperature-sensitive compounds. The expected correlation between altitude and temperature is found for soil and river material. The origin of river material is predominantly upstream soils and constant with river depth. Upon reaching the lowlands, input from weathered soils and lowland tributaries changed the compound distributions in the river main stem. Lowland soil input and/or in-river microbial production become an increasingly important source and overprint the mountain-sourced signal. Thus, the temperature-sensitive compounds appear to be useful to study carbon sources in mountain watersheds. Furthermore, comparing our data (headwaters) with the downstream Amazon River shows that lowland soils and/or in river production seem to dominate the signal finally exported to the ocean.

Key Points:
- Bacterial membrane lipids (brGDGTs) in soils from Madre de Dios catchment, Peru, record temperature
- The brGDGTs in river suspended matter reflect their catchment and accumulate downstream
- The brGDGTs primarily trace soil organic carbon in the Madre de Dios River system

Supporting Information:
- Supporting Information S1

Correspondence to:
F. M. S. A. Kirkels and F. Peterse,
f.m.s.a.kirkels@uu.nl;
f.peterse@uu.nl

Citation:
Kirkels, F. M. S. A., Ponton, C., Galy, V., West, A. J., Feakins, S. J., & Peterse, F. (2020). From Andes to Amazon: Assessing branched tetraether lipids as tracers for soil organic carbon in the Madre de Dios River system. *Journal of Geophysical Research: Biogeosciences*, *125*, e2019JG005270. https://doi.org/10.1029/2019JG005270

Received 20 MAY 2019
Accepted 12 NOV 2019
Accepted article online 19 DEC 2019

1. Introduction

The transport of organic carbon (OC) from soils to sea via rivers is a key process in the global carbon cycle, as terrestrial biospheric OC serves as a long-term sink of photosynthetically fixed CO_2 upon fluvial discharge and burial in marine sediments (Berner, 1982). The fluvial transport of terrestrial OC carries environmental signals from the catchment to depositional environments such as marine fans where they may be used for paleoclimate reconstructions (e.g., France-Lanord & Derry, 1994). To understand variations in the amount and composition of past and present terrestrial OC transport by rivers, as well as the climatic information they encode, it is important to assess the origin of the OC and processes it undergoes during transport.

Although lipid biomarkers make up only a minor part of OC, they are promising as tracers based on their source- or environmental-specific signature. A suite of bacterial membrane lipids, that is, branched glycerol dialkyl glycerol tetraethers (brGDGTs), has been proposed to serve as tracers of soil inputs into river systems (Hopmans et al., 2004; Weijers et al., 2006). The brGDGTs occur in soils worldwide and can vary in the number (four to six) and position (five or six) of methyl branches, as well as in the amount of cyclopentane moieties (up to two) incorporated in their structure, depending on the mean annual air temperature (MAT) and the pH of the soil in which they are produced (De Jonge, Hopmans, et al., 2014; Weijers, Schouten, et al., 2007). Hence, brGDGTs that are sequestered in sedimentary archives after erosion, runoff, and transport not only serve as tracers for soil OC but also contain information on (past) environmental conditions in the upstream catchment area (e.g., Bendle et al., 2010; Weijers, Schefuß, et al., 2007).

The interpretation of brGDGT-based paleorecords commonly assumes that brGDGTs in continental margin sediments approximate a uniform integration of the river basin. However, erosion may favor soil inputs, including brGDGTs, from specific parts of the catchment and various processes (e.g., in-river degradation, deposition or dynamic replacement), and may affect the fate of these compounds during transport (e.g., Bianchi et al., 2007; Cai et al., 1988; Mayorga et al., 2005; Onstad et al., 2000). As a result, we expect an evolving brGDGT signal during river transport. For instance, the distribution of brGDGTs in suspended particulate matter (SPM) in the Congo River was found to reflect different areas of the catchment at different times of the year, depending on the prevailing hydrological conditions (Hemingway et al., 2017). Hence, it is paramount to understand seasonal and sourcing effects on fluvially transported brGDGT signals.

Mountainous catchments present a highly erosive environment combined with a large temperature gradient, so that provenance changes can severely alter the environmental signal that is transferred by mountainous rivers. In the greater Amazon basin, explicit uncertainties exist on the contribution of Andean versus lowland-derived OC transported downstream. Bendle et al. (2010) analyzed brGDGTs in a 37 kyr sedimentary record from the Amazon River fan and observed an abrupt 10 °C drop in brGDGT-derived temperatures at the onset of the Holocene. Instead of a regional cooling, they hypothesized a sudden increase in contribution of brGDGTs from the Andean region, which is 11% of the Amazonian catchment by area and > 2,000 km distal along the meandering floodplain river. In contrast, studies of the modern-day Lower Amazon basin do not find an Andean signature and instead report that brGDGTs in SPM reflect mostly local soil input with additional in-river production (Kim et al., 2012; Zell, Kim, Abril, et al., 2013; Zell, Kim, Moreira-Turcq, et al., 2013). However, the integration and export of mountain signatures of brGDGTs has so far only been tested for the Alpine contribution to the modern Danube River, where the contribution of Alpine-derived brGDGTs appears negligible (Freymond et al., 2017, 2018), and as of yet data from Andean Rivers are lacking.

Another factor that may influence the brGDGT distribution archived in offshore sediments is in-river production (e.g., De Jonge, Stadnitskaia, et al., 2014; Kim et al., 2012; Zell, Kim, Abril, et al., 2013; Zell, Kim, Moreira-Turcq, et al., 2013; Zhu et al., 2011). In the Lower Amazon River, such an aquatic contribution caused a discrepancy of on average −2 °C between brGDGT-derived temperatures in SPM and the surrounding soils (Zell, Kim, Moreira-Turcq, et al., 2013). The magnitude of the offset likely varies spatially and temporally as there are seasonal and interannual variations in brGDGT production associated with hydrological dynamics (Kim et al., 2012; Zell, Kim, Abril, et al., 2013). Some recent progress has been made in untangling brGDGT sources in river SPM since De Jonge, Stadnitskaia, et al. (2014) found that aquatic brGDGTs can be recognized based on the abundance of 6-methyl brGDGTs relative to that of their 5-methyl isomers, quantified in the Isomer ratio (IR), with higher IR values indicating more aquatic production. Although several lowland rivers have been sampled to understand downstream brGDGT signals, mountain rivers have been less well studied, even though these systems supply sediment to archives of interest.

A fundamental step in identifying the provenance (i.e., source area within a river basin) of soil OC in rivers is to understand how brGDGTs associated with SPM are reflective of soils in the upstream catchment, and to what extent processes like hydrological dynamics (e.g., seasonality and preferential transport) and degradation or in situ production may introduce variability in the brGDGT signal. Therefore, in this study, we investigate brGDGT distributions in soils and SPM of the Madre de Dios River system, one of the upper tributaries in the Amazon River (Figure 1), to evaluate their suitability as specific tracers for soil OC during fluvial transport from a tropical montane watershed. The distinct wet and dry seasons and the ~3.5 km elevation

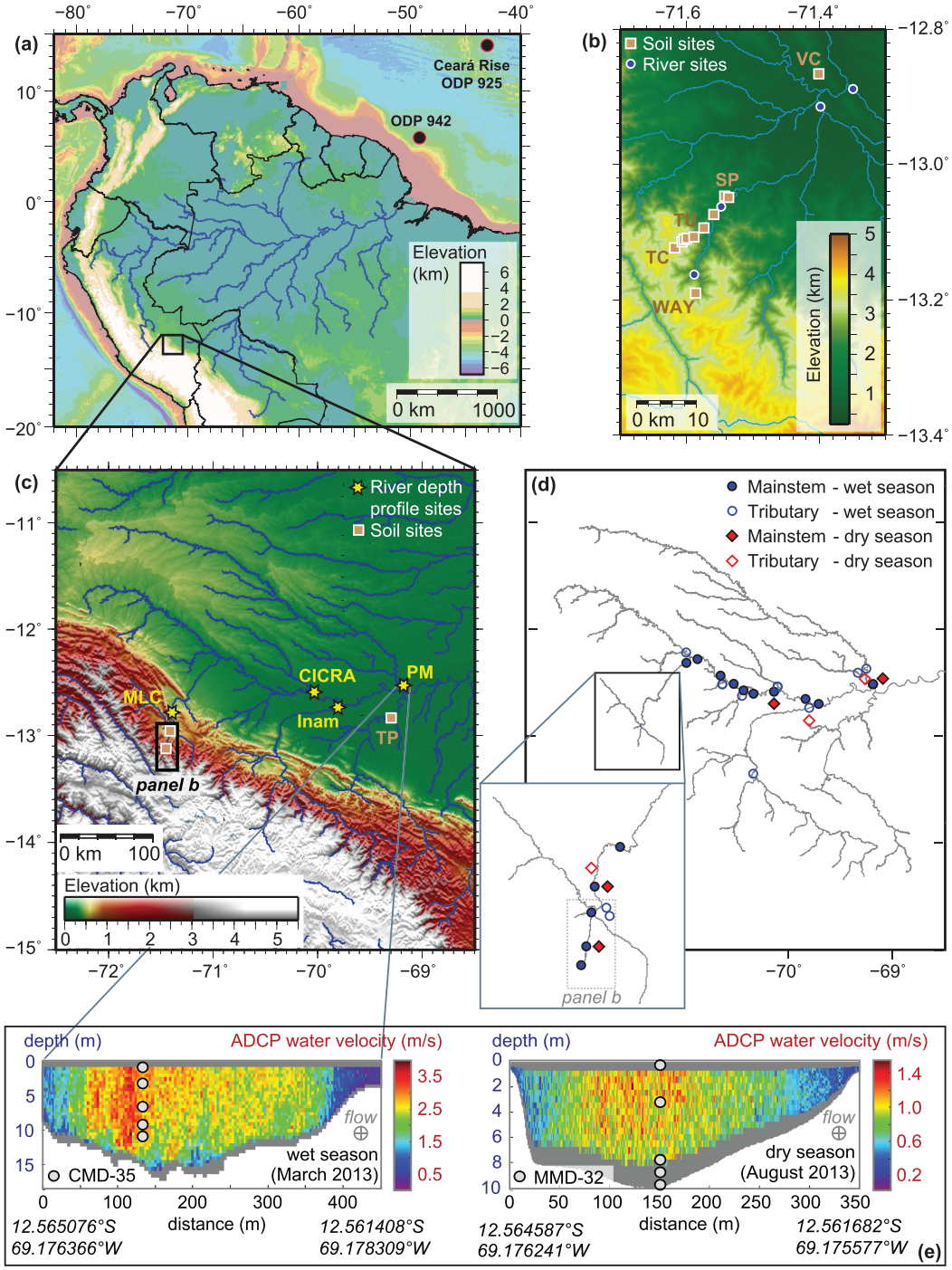

Figure 1. Shaded relief map showing (a) the position of the Madre de Dios River network in the larger Amazon basin, ODP site 925 at Ceará Rise (van Soelen et al., 2017) and ODP site 942 (Bendle et al., 2010), and the locations of part of the soil and river (depth profile) samples collected in the (b) Kosñipata River, which drains into the (c) Madre de Dios River. (d) Locations of river samples collected in the main stem (closed symbols) and tributaries (open) of the Kosñipata (inset) and Madre de Dios Rivers (main panel) during the wet (dark blue) and dry (red) seasons; a list of sample numbers can be found in Figure S1 in the supporting information. (e) Transect across the river at Puerto Maldonado showing river depth, Acoustic Doppler Current Profiler (ADCP) river flow velocity, and depth sampling locations (circles). River site abbreviations: MLC = Manu Learning Center (on the Madre de Dios River); CICRA = Centro de Investigación y Capacitación Río Los Amigos, also known as the CICRA-Los Amigos Biological Station (on the Madre de Dios River); Inam = Inambari River at Boca Inambari (tributary, just above confluence with the Madre de Dios River); PM = Puerto Maldonado (on the Madre de Dios River). Soil site abbreviations: WAY = Wayqecha; TC = Tres Cruces; SP = San Pedro; VC = Villa Carmen; TP = Tambopata (at Explorers' Inn along the Tambopata River).

gradient covered by the catchment provide contrasting conditions to study the transfer of brGDGTs from soils into the river and subsequent in-river (transport) processes. As brGDGTs have been shown to reflect the adiabatic cooling of air with increasing elevation in soils worldwide (e.g., Coffinet et al., 2017; Ernst et al., 2013; Sinninghe Damsté et al., 2008), comparison of brGDGT signatures in soils with those in river SPM will aid in determining the provenance of the heterogeneous OC pool carried by the river. Furthermore, differences in brGDGT signatures in SPM during wet and dry seasons can be used to evaluate the effects of (seasonal) changes in hydrological dynamics on the transport and sources of soil OC. Potential sorting effects on the brGDGT signature that will be delivered to the Amazon main stem can be assessed by examining the distribution and composition of brGDGTs in river depth profiles. Finally, by comparing the Madre de Dios data set with earlier studies on brGDGTs in the Lower Amazon River we can gain insight into the fate of brGDGTs in the greater Amazon basin along the soil-river-ocean continuum. At the same time, our knowledge on the provenance and behavior of brGDGTs along the transport pathway from soils to sea (source to sink) will aid in interpreting paleo-environmental reconstructions based on brGDGTs in river-supplied marine sedimentary records, such as those from the Amazon fan.

2. Materials and Methods

2.1. Madre de Dios River Basin

The Madre de Dios River system, with its headwaters in the Kosñipata River in the upper Andean section, is a tributary of the Amazon River, draining the southern Peruvian Andes (Figure 1). The Madre de Dios and other Andean-sourced tributaries of the Amazon River are "white water" rivers that carry high levels of suspended sediments due to mechanical erosion of the Andean Mountain chain (Meade et al., 1985). Hence, the Andean headwaters are very important for sediment production and downriver transport of associated soil OC in the Amazon basin, compared to the "black water" (high dissolved OC concentrations) and "clear water" (high phytoplankton production) tributaries in the lowlands (McClain & Naiman, 2008). In the Madre de Dios catchment, vegetation changes from puna (high-elevation grasslands) above the treeline to tropical montane cloud forest—recognized as special biodiversity hot spot (e.g., Asner et al., 2015; Hoorn et al., 2010) —at mid-elevations and moist tropical rainforest in the lowlands (Clark et al., 2016). OC stored in soils increases toward high-elevation sites due to reduced decomposition rates (low pH and colder conditions) and a higher input (Zimmermann et al., 2009); this trend is reflected by an increase in the depth of the O-horizon with elevation (Feng et al., 2016). Soil OC is mostly contained as detritus (i.e., unprotected, particulate OC) at high elevations, whereas in the lowlands OC is more associated with mineral phases and protected in aggregates (Zimmermann, Leifeld, et al., 2010). The lowland portion of the Madre de Dios watershed is here defined as <500 m asl, where the river has extensive floodplains and shows high rates of lateral channel migration/meandering cutting through alluvial deposits with geomorphological features as oxbow lakes and levees (Hamilton et al., 2007; Householder et al., 2012). The Andean part (>500 m asl) includes the submontane, montane, and high-Andean regions that are characteristically distinct based on biogeography and climatology (Eva & Huber, 2005). Erosion in the Madre de Dios headwaters is enhanced by steep hillslopes and occurs via two main geomorphic mechanisms (i) bedrock landslides that mobilize material ranging from fine-grained OC to entire tree trunks and (ii) shallow landslides and overland flow that move OC from surface soils, combined they result in efficient hillslope-river coupling (Clark et al., 2016, 2017). At lower elevations (i.e., downstream of San Pedro, < 1,500 asl) alluvial sediment deposits are found (Clark et al., 2017), suggesting a transient OC sink, but the role of channel migration and floodplain storage on soil-river connectivity in the lowlands remains to be assessed in detail (Torres et al., 2017).

Erosion and river sediment transport in the modern Madre de Dios watershed are driven by precipitation and geological uplift of the Andes (Clark et al., 2016, 2017). The South American low level jet carries humid winds westward over the Amazon basin and then along the Andean Mountain flanks, driving orographic rainfall over the eastern side of the Andes (Espinoza et al., 2015; Marengo et al., 2004). Changes in the position of the Intertropical Convergence Zone (ITCZ) result in pronounced seasonality in the precipitation regime (Killeen et al., 2007). Consequently, the Madre de Dios River is characterized by significant (~5 m, max. 8 m) water level changes (atrium.andesamazon.org) between the dry (May–September) and wet (December–March) season (Clark et al., 2017), and sediment loads increased from 0.03–1.39 g/L for surface waters in the dry season up to 6.46–63.36 g/L in the Andes (near Wayqecha at ~3,025 m asl) during the wet season (Feng et al., 2016). Mean annual precipitation in the catchment increases with elevation along the

Andean foreland, reaches a maximum of >5,000 mm/year at 1,500 m asl, and then decreases progressively to ~1,000 mm/year above 4,100 m (Rapp & Silman, 2012). The mean air temperature (MAT) decreases from 24.0 °C near Tambopata in the lowlands (~230 m asl, 2003–2008; atrium.andesamazon.org) to 6.5 °C at the highest elevation site near Tres Cruces (~3,600 m asl, 2007–2008; Rapp & Silman, 2012), generally following the trend of adiabatic cooling of air. Rapp and Silman (2012) report a mean yearly lapse rate of −5.3 °C/km for the Kosñipata valley, which is broadly representative of the upland Madre de Dios catchment. The higher mean temperature and smaller diurnal temperature cycles in the wet season in the Andean part imply a seasonal change in lapse rate (i.e., greater cooling with altitude in the wet season) (Rapp & Silman, 2012).

2.2. Soil Sampling

Soils were collected along an elevation gradient from 194 to 3,644 m asl (Figure 1), in December 2010 from well-studied, representative plots in the catchment (see Nottingham, Turner, et al., 2015; Nottingham, Whitaker, et al., 2015). From each plot, organic (O) and mineral (M) soil layers were taken from five symmetrically distributed 40 × 40 m subplots and then combined. The soils classify as Umbrisols at sites above 2,720 m; Cambisols from 1,000 to 2,020 m; and Haplic Cambisol, Haplic Alisol, and Haplic Gleysol (with intermittent stagnant water conditions) at the lowland sites (Nottingham, Turner, et al., 2015; Quesada et al., 2010). The thickness of the organic layer varies across the catchment, and the mineral soil layer starts at depths ranging from 23 cm in the Andean uplands to 1 cm below the surface in the lowlands (Nottingham, Whitaker, et al., 2015). Where the O-horizon was >10 cm, the top 10 cm was sampled; otherwise, the entire O-horizon present was collected. For the M-horizon only the upper 10 cm was taken. The soil samples were dried and homogenized prior to analyses.

2.3. River SPM Sampling

The SPM was sampled from the Kosñipata-Madre de Dios River in March (wet season) and August (dry season) 2013 along an elevation gradient of ~3,500 m, spanning the transition from the upper Andes to the Amazonian lowlands. At each location, 60–180 L of surface water was collected by immersion of a 10 L bucket. Locations at high elevation were accessed via the riverbanks, while at lower stations water was collected from a boat at the point of highest flow velocity in the channel based on Acoustic Doppler Current Profiler transects. In addition, river depth profiles (2–5 depths per site) were sampled during both wet and dry seasons near Puerto Maldonado (1,180 m mean catchment elevation) and near CICRA-Los Amigos Biological Station (822 m mean catchment elevation) in the Madre de Dios main stem (Figure 1). Two additional depth profiles were collected from the upper Madre de Dios main stem (2,012 m mean catchment elevation) and the Inambari tributary (2,777 m mean catchment elevation) during the wet season only (Figure 1).

All river water samples were transferred into wine bags (ethylene-vinyl alcohol: EVOH) and filtered within 12 h through 0.2 μm polyethyl sulfone (PES) filters using pressurized filter units operated by a bicycle pump (after Galy et al., 2007). Filters containing SPM were stored cool in Whirlpak™ bags for transport. In the laboratory, SPM was recovered from the filter by rinsing with milliQ water and the obtained material was freeze-dried.

2.4. Sample Elevation

River SPM is sourced from the catchment upstream of the sampling site. To determine the mean elevation of the area represented by each SPM sample, a flow-routing algorithm in Geographic Resources Analysis Support System within Geographic Information Software was used, using Shuttle Radar Topography Mission-derived digital elevation data with a spatial resolution of 3 arc sec (~90 m). For the soils the actual sampling elevation is used.

2.5. Geochemical and Meteorological Data

Grain size, sediment load, and mineral specific surface area (SSA) of the SPM, total OC (TOC) contents of both SPM and soils, and soil pH were previously reported (Feng et al., 2016; Nottingham, Whitaker, et al., 2015). Meteorological data were reported by Rapp and Silman (2012) using weather stations at (or nearby) soil sampling sites. Stations located at Wayqecha (3,025 m asl) and Tambopata (230 m asl, used for estimates

for TP3 and TP4) were situated in open field conditions and thus may slightly overestimate MAT relative to the soil sites that were situated under forest canopy.

2.6. GDGT Extraction and Analysis

Soils and SPM were extracted with dichloromethane (DCM):methanol (MeOH) (9:1, *v*:*v*) using an Accelerated Solvent Extraction system (ASE 350, Dionex) at 100 °C and 1500 psi. The total lipid extract was separated into a neutral and acid fraction by column chromatography (5 cm × 40 mm Pasteur pipette, NH_2 sepra bulk packing, 60 Å) eluting with 2:1 DCM:isopropanol, as described in Ponton et al. (2014). The neutral fraction was dried under an N_2 flow at 35 °C and passed over a second column with 5% deactivated silica gel (Pasteur pipette, 100–200 mesh) using ~5 mL hexane, ~5 mL DCM, and ~3 mL MeOH as sequential eluents. Each fraction was subsequently dried under N_2 for refrigerated storage and shipped for analysis.

A known amount of synthetic C_{46} glycerol trialkyl glycerol tetraether was added to the DCM fraction as an internal standard (after Huguet et al., 2006). The fraction was then redissolved in hexane:isopropanol (99:1, *v*:*v*) and passed through a 0.45 μm polytetrafluoroethylene (PTFE) filter. The GDGTs were analyzed using Ultra High Performance Liquid Chromatography-Atmospheric Pressure Chemical Ionization Mass Spectrometry (UHPLC-APCI-MS) with an Agilent 1260 Infinity coupled to an Agilent 6130 quadrupole mass spectrometer (Agilent Technologies, Santa Clara, CA, USA) at Utrecht University, following Hopmans et al. (2016). In short, separation of GDGTs was achieved on two silica Waters Acquity UPLC BEH Hilic columns (150 × 2.1 mm; 1.7 μm; Waters corp., Miliford, MA, USA) at 30 °C, preceded by a guard column of the same material. Elution was isocratic using 82% A and 18% B for 25 min, followed by a linear gradient to 70% A for 25 min, and then to 100% B in 30 min, with a flow rate of 0.2 mL/min and injection volume of 10 μL, where A = hexane and B = hexane:isopropanol (9:1, *v*:*v*). Each run was followed by a 20 min equilibrium phase. Conditions for APCI-MS were nebulizer pressure 60 psi, vaporizer temperature 400 °C, drying gas (N_2) flow 6 L/min and gas temperature 200 °C, capillary voltage 3500 V, and corona 5.0 μA.

Detection of GDGTs was accomplished in selected ion monitoring mode, targeting the protonated molecules $[M + H]^+$. Agilent Chemstation software B.04.03 was used to integrate peak areas in the mass chromatograms. Concentrations (semiquantitative) were calculated by comparing the integrated signal of the respective compound with that of the internal standard. The response factor between the respective brGDGT compound and internal standard was assumed to be 1:1.

2.7. Calculation of GDGT-Based Indices

Several indices are used to determine the sources and fate of brGDGTs in transit, and thus the suitability of brGDGTs as tracers for soil OC in the Madre de Dios River system. Roman numerals refer to the molecular structures shown in De Jonge, Hopmans, et al. (2014). The branched and isoprenoid tetraether (BIT) index was calculated following Hopmans et al. (2004), including 6-methyl brGDGTs:

$$\text{BIT index} = (\text{Ia} + \text{IIa} + \text{IIa}' + \text{IIIa} + \text{IIIa}')/(\text{Ia} + \text{IIa} + \text{IIa}' + \text{IIIa} + \text{IIIa}' + \text{crenarchaeol})$$

Soil pH was reconstructed using the cyclization of branched tetraethers (CBT′) index and the transfer function of De Jonge, Hopmans, et al. (2014), using the fractional abundances of brGDGTs:

$$\text{CBT}' = {}^{10}\log((\text{Ic} + \text{IIa}' + \text{IIb}' + \text{IIc}' + \text{IIIa}' + \text{IIIb}' + \text{IIIc}')/(\text{Ia} + \text{IIa} + \text{IIIa}))$$

$$\text{pH} = 7.15 + 1.59*\text{CBT}'$$

Similarly, the degree of methylation ($\text{MBT}'_{5\text{methyl}}$) is based on

$$\text{MBT}'_{5\text{methyl}} = (\text{Ia} + \text{Ib} + \text{Ic})/(\text{Ia} + \text{Ib} + \text{Ic} + \text{IIa} + \text{IIb} + \text{IIc} + \text{IIIa})$$

and mean air temperatures were estimated using fractional abundances of brGDGTs and the transfer function based on multiple linear regression (MAT_{mr}; De Jonge, Hopmans, et al., 2014):

$$\text{MAT}_{\text{mr}} = 7.17 + 17.1*\text{Ia} + 25.9*\text{Ib} + 34.4*\text{Ic}–28.6*\text{IIa}$$

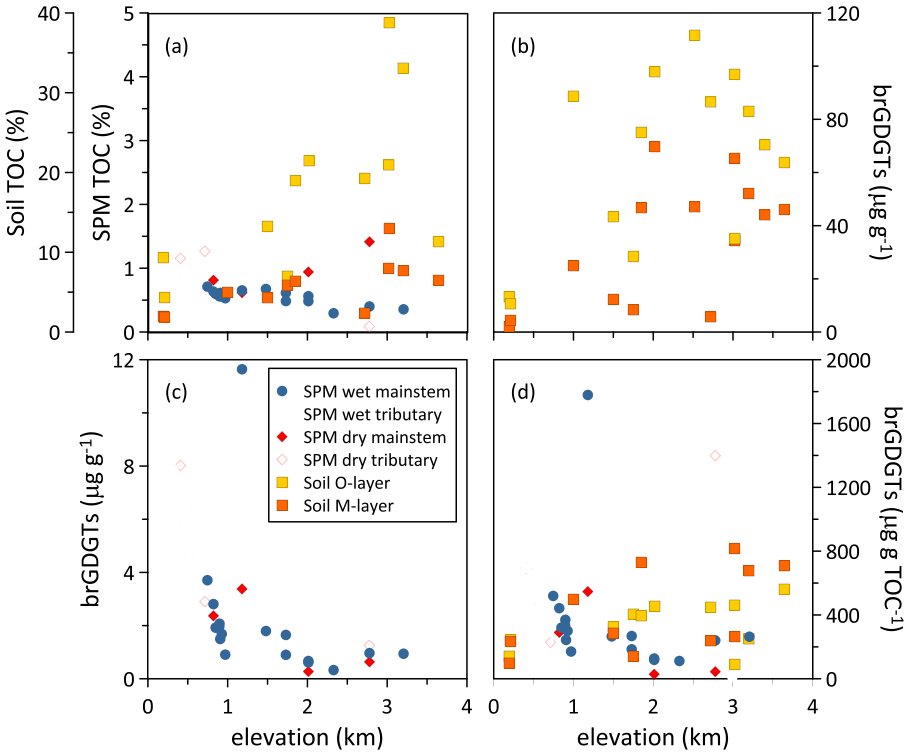

Figure 2. Changes with elevation in (a) TOC of soil and SPM, (b) brGDGT concentration in soil, (c) brGDGT concentration in SPM, and (d) TOC-normalized brGDGT concentrations in soil and SPM. Elevation is the sampling elevation for soils and mean catchment elevation for SPM.

The Isomer Ratio (IR) represents the relative abundance of penta- and hexamethylated 6-methyl brGDGTs versus the total (5-methyl and 6-methyl) penta- and hexamethylated brGDGTs (Dang et al., 2016; modified from De Jonge, Stadnitskaia, et al., 2014):

$$\mathrm{IR} = (\mathrm{IIa}' + \mathrm{IIb}' + \mathrm{IIc}' + \mathrm{IIIa}' + \mathrm{IIIb}' + \mathrm{IIIc}')/(\mathrm{IIa} + \mathrm{IIb} + \mathrm{IIc} + \mathrm{IIIa} + \mathrm{IIIb} + \mathrm{IIIc} + \mathrm{IIa}' + \mathrm{IIb}' + \mathrm{IIc}' + \mathrm{IIIa}' + \mathrm{IIIb}' + \mathrm{IIIc}')$$

The degree of cyclization (DC) was calculated according to Sinninghe Damsté et al. (2009), including 6-methyl brGDGTs:

$$\mathrm{DC} = (\mathrm{Ib} + \mathrm{IIb} + \mathrm{IIb}')/(\mathrm{Ia} + \mathrm{Ib} + \mathrm{IIa} + \mathrm{IIa}' + \mathrm{IIb} + \mathrm{IIb}')$$

3. Results and Discussion

3.1. Soil OC Characteristics

Bulk OC properties of the soils along the elevation transect have been reported and discussed in detail previously (Feng et al., 2016; Nottingham, Turner, et al., 2015; Nottingham, Whitaker, et al., 2015). In short, the soils from this study are acidic and have pH values ~4 (Nottingham, Whitaker, et al., 2015), with limited variation across the catchment (supporting information: Kirkels et al., 2019, https://doi.pangaea.de/10.1594/PANGAEA.906170). The TOC content varies between 4.3 and 38.8% in the organic layers (n = 11), and 1.9 and 13.0% in the mineral horizons (n = 11), both increasing with elevation (Figure 2a; Feng et al., 2016). Although net primary production decreases with elevation (Girardin et al., 2014; Huasco et al., 2014; Malhi et al., 2014), reduced decomposition at lower temperatures may explain the soil OC accumulation at high elevations (Zimmermann, Meir, et al., 2010).

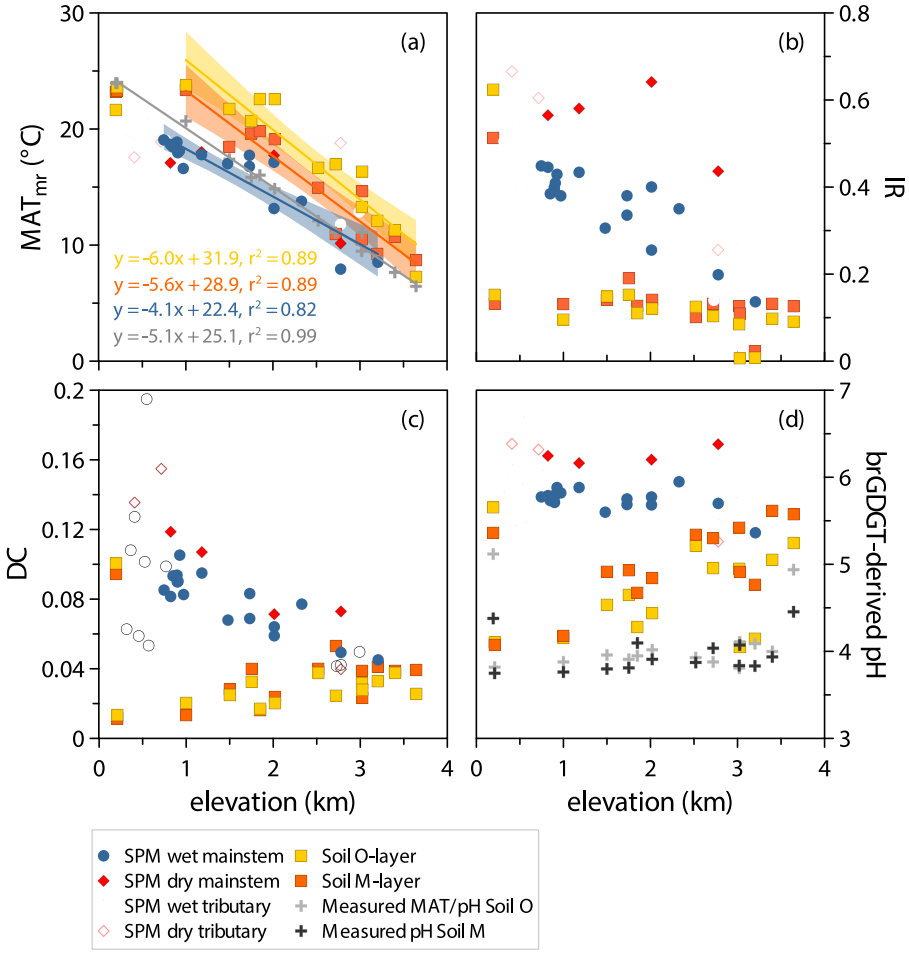

Figure 3. Changes with elevation in (a) reconstructed temperatures (MAT_{mr}), (b) the isomerization ratio (IR), (c) the degree of cyclization (DC), and (d) reconstructed pH based on brGDGTs in SPM and soils. Elevation is the sampling elevation for soils and mean catchment elevation for SPM. Lines represent linear regression with 95% confidence intervals for organic and mineral soil horizons (for the Andean part of the catchment, excluding lowland soils TP3 and TP4), wet season SPM, and measured soil temperatures.

3.2. BrGDGTs in the Andes-Amazon Soil Transect

The brGDGT concentrations in the catchment soils are 10.7–111.7 μg/g soil (91–563 μg/g OC) in the organic horizons and 2.0–69.7 μg/g soil (99-817 μg/g OC) in the mineral layers (Figure 2b). The relative distribution of brGDGTs in the soils translates into reconstructed MATs between 7.3 and 23.8 °C in the O-horizons and 8.7 and 23.4 °C in the mineral soil layers, which is in the same range as MATs measured by temperature loggers along the transect (6.5–24.0 °C; Figure 3a). The reconstructed MATs show a good correlation with elevation (r^2 = 0.89 for both O- and M-horizons; Figure 3a) in the Andean part of the catchment (> 500 m asl) and track the expected adiabatic temperature response to altitude, similar to brGDGTs in soils along elevation transects in other regions worldwide (e.g., Ernst et al., 2013; Nieto-Moreno et al., 2016; Sinninghe Damsté et al., 2008). The temperature lapse rates based on brGDGTs in the organic (−6.0 °C/km) and mineral (−5.6 °C/km) soil layers are slightly higher than that measured by the temperature loggers (−5.1 °C/km, r^2 = 0.99) for the Andean part of the catchment (Figure 3a).

MATs are particularly overestimated between 1 and 3 km elevation, and although the offset is within the uncertainty of the proxy (4.6 °C, De Jonge, Hopmans, et al., 2014), the consistent trend warrants further investigation. Deng et al. (2016) reported a similar overestimation of reconstructed MATs for high-elevation soils at the Tibetan Plateau and linked this to systematic changes in the seasonal contrast in temperature and hydrology with elevation, further amplified by the monsoon climate. They suggest that brGDGTs are

preferentially produced during the wet (summer) season given the unfavorable growth conditions during the dry season. Hence, the timing and length of the wet season in the Madre de Dios catchment likely contribute to the bias in brGDGT-based MATs toward higher rainy season temperatures in the Andean section. The higher mean temperature and smaller diurnal cycles in the Madre de Dios wet season (Rapp & Silman, 2012) may further favor brGDGT production. On the other hand, for the Argentinean high Andes, Nieto-Moreno et al. (2016) found that brGDGTs underestimated measured MAT and deviated toward dry season temperatures when soil moisture levels were speculated to be high after the rainy season, pointing out that mechanisms driving brGDGT production along elevation gradients are not yet fully understood. Studies on low-altitude and mid-altitude soils (< 1,800 m asl) in temperate, dry continental and subhumid climates (Lei et al., 2016; Weijers et al., 2011; Zang et al., 2018) report no seasonal bias, probably due to sufficient rainfall in all seasons that allows for brGDGT production throughout the year. We note that, besides changes in temperature and moisture availability along elevation gradients, environmental shifts in microbial composition, vegetation, and/or soil type may further influence brGDGT production. For instance, for tropical elevation gradients overestimation by reconstructed MATs was previously noted using an earlier transfer function (Ernst et al., 2013; Sinninghe Damsté et al., 2008) and explained by potential differences in the temperature sensitivity of brGDGT producers on a global versus local scale and shifts in vegetation type.

In the lowlands, where temperature and moisture are more stable and thus unlikely to be limiting factors for brGDGT-producing organisms, reconstructed MATs of the O- and M-horizons closely resemble the measured temperature (Figure 3a). Nevertheless, the apparent flattening of the trend in reconstructed MAT with elevation at the transition from the Andean to the lowland part of the Madre de Dios catchment (at ~500 m asl) may also be an artifact of the near saturation of the proxy. This is manifested in the dominance of brGDGT Ia in the lowlands and consequently results in a reconstructed MAT of maximal ~25 °C using the transfer function of De Jonge, Hopmans, et al. (2014). For the Amazon lowlands where MAT is generally ≥25 °C, saturation of the proxy would imply that there is little sensitivity to assess sourcing from lowland regions in the downstream river.

The brGDGT distributions generally also vary with the pH of the soils, reflected by the degree of cyclization and the relative abundance of 6-methyl brGDGT isomers, quantified as DC and IR, respectively (De Jonge, Hopmans, et al., 2014; Sinninghe Damsté et al., 2009; Weijers, Schouten, et al., 2007). In the Madre de Dios transect, the overall low soil pH is reflected by the low abundance of 6-methyl brGDGTs, resulting in IR values <0.20 for all soils, except for the periodically inundated soil at 194 m asl (TP4) that has much higher IR values (Figure 3b). Similarly, the DC is typically below 0.04 for all soils, except for TP4 (Figure 3c). Despite the relatively stable IR and DC, brGDGT-derived pH values vary between 4.1 and 5.7 and show a general increase toward higher elevation (Figure 3d). The absence of corresponding variation in measured soil pH suggests that the incorporation of rings into soil-derived tetraether lipids and occurrence of 6-methyl isomers in soils are additionally driven by an environmental control that covaries with elevation.

The distinct brGDGT distribution in the lowland soil TP4 may be explained by its location near the meandering river. The soil type (gleysol) indicates that this site is frequently flooded and experiences soil-river exchange. These waterlogged soils are abundantly found in a narrow zone of presently active river floodplains and riverbanks along lowland tributaries and the downstream Amazon River (Hamilton et al., 2007; Osher & Buol, 1998). On the other hand, more distal floodplains that are not subjected to overbank flow during river pulses in the lowland portion of the Madre de Dios basin (e.g., TP3 in this study; Peru-10 in De Jonge, Hopmans, et al., 2014) and north Peruvian lowland soils near the Amazon River main stem (De Jonge, Hopmans, et al., 2014) have no deviating brGDGT distributions and are characterized by typically low IR and DC values (<0.2 and <0.01, respectively).

3.3. Physiochemical Characteristics of SPM in Surface Waters

As previously described by Feng et al. (2016), the sediment load in the surface waters of the Madre de Dios River system ranges between 0.23 and 63.36 g/L during the wet season, and between 0.03 to 1.39 g/L during the dry season (Kirkels et al., 2019). The sediment load is generally higher than that reported for other mountain headwaters of the Amazon River (0.6–2 g/L; Aufdenkampe et al., 2007; Hedges et al., 2000; Townsend-Small et al., 2008), highlighting the relative importance of the Madre de Dios River system to the contribution of sediment from the Andes to the main stem Amazon River (Clark et al., 2017).

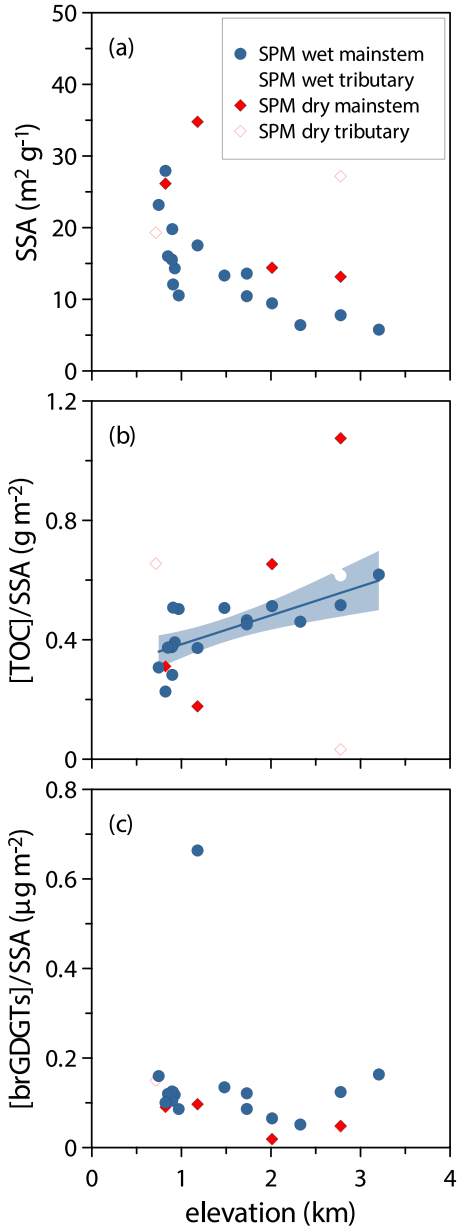

Figure 4. (a) Change in specific surface area (SSA) of SPM with elevation, (b) [TOC]/SSA with elevation, and (c) [brGDGTs]/SSA with elevation. Elevation is the sampling elevation for soils and mean catchment elevation for SPM. Line represents linear regression with 95% confidence intervals for TOC/SSA.

The modal grain size of the SPM is dominated by the silt fraction and is relatively invariant along the transect, whereas the SSA increases downstream, with a SSA of 7.8 m^2/g in the Andean sector at San Pedro (~2,800 m mean catchment elevation) and 28.0 m^2/g in the floodplain river near Puerto Maldonado (~800 m mean catchment elevation) in the wet season, and, respectively, 13.2 and 34.8 m^2/g in the dry season (Figure 4a; Feng et al., 2016). Maximum SSA values of up to 40.4 m^2/g were observed in lowland tributaries (~400 m mean catchment elevation) in the wet season.

The OC content of SPM in the main stem samples ranges from 0.3 to 0.71% during the wet season and increases toward the Amazon lowlands (Figure 2a). This downstream increase in OC content of SPM is opposite to the trend in soil OC (i.e., organic-rich soils at high elevation) and can be explained by a dilution effect, as intense erosion in the upper Andes results in large inputs of mineral matter into the river (McClain & Naiman, 2008; Townsend-Small et al., 2008). The OC content of SPM in the main stem is more variable during the dry season and ranges from 0.62 to 1.42%. The somewhat higher values compared to the wet season are due to lower sediment yields, and thus reduced mineral input and less dilution of the OC content. SPM OC content in the Madre de Dios River is at the lower end of the range observed for other Amazonian headwaters (0.6–30.3%, Aufdenkampe et al., 2007; ~ 0.5–60%, Townsend-Small et al., 2008) but generally comparable with that in the Lower Amazon River (0.6–2.22%, Bouchez et al., 2014; 1–4%, Kim et al., 2012).

Normalizing the OC content to SSA may give insights into preservation and/or degradation of OC during transit (Figure 4b; Keil et al., 1997). In this view, the decrease in [TOC]/SSA ([TOC], i.e. concentration, normalized to *g* sediment) observed with lowering elevation in the Madre de Dios River is generally interpreted as protection of OC by its association with mineral surfaces in the Andean part of the river, whereas the lower values in the lower main stem and lowland tributaries would reflect the increased exposure to oxygen and subsequent remineralization (Blair & Aller, 2012; Mayer, 1994). However, changes in SSA and [TOC] may also be driven by differences in mineralogy, and by OC transport and binding mechanisms, without direct dependency between SSA and [TOC] at the catchment scale.

In the downstream Madre de Dios, Guyot et al. (2007) reported relatively high levels of smectite compared to other Andean headwaters. Particularly, the lowland tributaries account for high SSA values in wet season SPM (Figure 4a), linked with the presence of secondary clays in lowland soils (Osher & Buol, 1998). Given the high SSA of smectite, a small contribution to the clay mixture may (largely) impact SSA but not TOC. Similarly, Galy et al. (2008) found for the Ganges-Brahmaputra River that differences in SSA were solely due to a different clay composition (i.e., a higher proportion of smectite in the Ganges compared to the Brahmaputra) at similar TOC levels. The downstream increase in SSA for the Madre de Dios is consistent with the geographical setting of the lowlands where episodic flooding of areas near the river channel governs repeated deposition and mobilization of young, fine-textured alluvium (Hamilton et al., 2007; Osher & Buol, 1998; Rigsby et al., 2009), in combination with active weathering of rejuvenated (topsoil removed by erosion) soils (Chadwick & Asner, 2016; Quesada et al., 2010).

On the other hand, TOC in the Madre de Dios SPM may behave independently of SSA due to the presence of detrital OC. In the Andean headwaters, unselective erosion by predominant landslides (Clark et al., 2017) in combination with a large part of soil OC stocks contained as detritus that is not associated with the mineral

fraction (Zimmermann, Leifeld, et al., 2010) could mean that the abundance of [TOC] in the upland river is not controlled by SSA. This would imply decoupled transport of unbound, detrital OC and mineral-associated OC—the latter being more prevalent in the lowlands where soil OC stocks are predominantly mineral bound (Zimmermann, Leifeld, et al., 2010). The shift from detrital to mineral-associated OC from the Andes to the lowlands may also explain the decreasing discrepancy between soil and wet season SPM OC content (Figure 2a), indicating that SPM is mostly derived from mineral-associated OC. Bouchez et al. (2014) suggested that detrital OC in the Lower Amazon River may be more buoyant and therefore transported differently near the channel surface compared to the SPM-OC fraction.

3.4. BrGDGT Concentrations in Surface Waters

The concentrations of brGDGTs in SPM from the surface waters of the Madre de Dios main stem and tributaries range from 0.45 to 11.6 μg/g during the wet season. Concentrations are relatively invariant in the upper catchment but increase from around 1,000 m asl toward the lowlands (Figure 2c). During the dry season, brGDGT concentrations vary between 0.28 and 8.0 μg/g and follow the trend of the wet season. Since the OC content of SPM also slightly increases downstream (Figure 2a), brGDGT concentrations are normalized to OC to further investigate this trend. OC-normalized brGDGT concentrations increase downstream from 12 to 801 μg/g OC in the wet season (with an outlier of 1,780 μg/g OC for CMD35, at a mean elevation of 1,180 m), indicating that brGDGTs make up an increasingly larger part of the OC toward lower elevation (Figure 2d). Subsequent normalization of brGDGT concentrations to SSA shows that [brGDGTs]/SSA fluctuates between 0.05 and 0.14 $\mu g/m^2$ (with an outlier of 0.66 $\mu g/m^2$ again at CDM35; Figure 4c). For comparison, these concentrations are 2 orders of magnitude higher than the window of 17–71 ng/m^2 proposed for "typical rivers" based on brGDGTs in the Danube River (Freymond et al., 2018). The distinct evolution of SSA-associated OC and brGDGTs with elevation in the Madre de Dios system may be explained by a transition of OC from the particulate into the dissolved phase in combination with a large quantitative input from lowland soils driving the downstream decrease in [TOC]/SSA. Feng et al. (2016) analyzed dissolved organic carbon (DOC) concentrations in the Madre de Dios River during the wet season and found values between 0.03 and 0.2 mg/L. Although these concentrations are low compared to other Andean headwaters (~1–4 mg/L, Guyot & Wasson, 1994; Hedges et al., 2000; 0.7–6.1 mg/L, Townsend-Small et al., 2005), they do increase in downstream direction, particularly upon reaching the lowlands. This typical increase in DOC concentrations upon entering the lowlands was observed in other tributaries draining the Andes (Guyot & Wasson, 1994; Hedges et al., 2000) and attributed to regular flooding of the riparian zone, thus maximizing connectivity between river and floodplains. The hydrophobic nature of brGDGTs would then cause their downstream enrichment in the SPM OC fraction. In addition, other factors, such as an overprint by in situ produced brGDGTs in the river (e.g., De Jonge, Stadnitskaia, et al., 2014; Zell, Kim, Moreira-Turcq, et al., 2013) or hydrological sorting and/or preferential preservation (e.g., Goñi et al., 1997; Prahl et al., 1994), could contribute to the downstream accumulation of brGDGTs. The influence of these processes may be recognized by changes in the brGDGT signature downstream and/or along depth profiles in the river.

3.5. Evolution of brGDGTs Signatures in Surface Water During Transport

The brGDGT signature in the main stem SPM changes with elevation, translating into temperatures from 7.9 °C in the Andes to 19.1 °C in the lowlands during the wet season, and from 10.2 °C to 18.0 °C during the dry season (Figure 3a). Similar to the brGDGTs in soils, there is a clear manifestation of the elevation gradient in the SPM, particularly during the wet season, with a lapse rate of −4.1 °C/km elevation ($r^2 = 0.88$, $p < 0.001$). This trend suggests that there is a continuous addition of soil material to the SPM along the gradient. The lower intercept of the SPM-based lapse rate compared to that of the soil-based lapse rates, together with the accumulation of brGDGTs in SPM, indicates that brGDGTs in the river integrate the signature of upstream soils and suggests relative persistence of soil-derived brGDGTs during river transport. In contrast, plant waxes carried by the Madre de Dios (Feakins et al., 2018; Ponton et al., 2014) were found undergo mineralization and replacement in transit and thus export no predominantly Andean signal.

Beyond the brGDGT-based temperature-altitude correlations observed in both SPM and soils, the brGDGT signature in SPM deviates from that in the soils based on the relative amount of 6-methyl isomers (quantified in the IR), as well as in their degree of cyclization (DC) (Figures 3b and 3c). De Jonge, Stadnitskaia, et al. (2014) suggested that a high relative abundance of 6-methyl isomers in rivers may be indicative of in situ production, based on higher IR values for SPM in the Yenisei River compared to those in soils. In the Madre de

Dios basin, soils have low and relatively invariable IR values (<0.20) along the altitudinal gradient, whereas the IR in SPM increases from 0.14 in the Andes to 0.67 in the lowlands (Figure 3b). The high flow velocity in combination with high sediment load and thus turbid water is unfavorable for primary production in the upstream river (Wissmar et al., 1981), but conditions likely improve downstream (e.g., higher temperature and lower flow velocity) and may stimulate in-river production. Similarly, the DC of brGDGTs increases with decreasing elevation more for SPM than for soils, although the range of variation is minor (<0.2; Figure 3c). In addition, the BIT index was calculated that was initially developed to determine the input of soil OC into the marine environment (high vs low values for soil vs aquatic sources), but it is also influenced by crenarchaeol produced in rivers (e.g., Kim et al., 2012; Zell, Kim, Moreira-Turcq, et al., 2013). The BIT index of the soils in the Madre de Dios catchment is close to 1, as a result of the near absence of crenarchaeol in these soils and in low pH soils in general (Weijers et al., 2006). Also in SPM the BIT index is high and varies between 0.90–0.98 and 0.89–0.94 during the wet and dry seasons, respectively, where the slightly lower SPM BIT values indicate that some in situ riverine production is taking place. Together, this suggests an increasing contribution of mainly 6-methyl brGDGTs during lowland fluvial transport, especially during the dry season, when slower flow velocities may favor more in-river production.

Alternatively, the lowland soil TP4, which is dynamically influenced by flooding and river erosion/deposition as part of the active riverbank/floodplain, gives insight in another mechanism that may explain the increase in IR and DC downstream, especially in the wet season. This soil has IR and DC ratios that are very similar to that of SPM (Figures 3b and 3c), which can be explained by the deposition of SPM onto the soil and/or by the production of "SPM-like" brGDGTs within the inundated soil. Comparable brGDGT signals in SPM and inundated riverbank soils have also been reported for the Lower Amazon River (Zell, Kim, Abril, et al., 2013). Hence, if river SPM in the lowlands is primarily sourced from active riverbank/floodplain soils like TP4, the changing ratios may also reflect local soil-to-river input from this temporarily flooded zone near the river channel rather than true in-river production. A dominant contribution of riverbank/floodplain material is in line with model predications for meandering river systems—this is attributed to active floodplain exchange and preferential mobilization of young deposits, thus overprinting biomarker signals downstream (Torres et al., 2017).

In an attempt to roughly estimate the contributions of soil-derived and in situ produced brGDGTs to SPM, we here assume that the relative abundance of 6-methyl brGDGTs is representative of in-river production (including potential production in inundated floodplains as discussed above). SPM in the dry season—when production within the water column will likely be maximal—indeed has the highest IR value and thus will be used as end-member for in-river production ($IR_{in\text{-}river} = 0.67$) in a simple binary mixing model (modified after Kim et al., 2012):

$$f_{\text{in-river}} = \frac{IR_{SPM(sample)} - IR_{Soil}}{IR_{in-river} - IR_{Soil}}$$

where $f_{in\text{-}river}$ (fraction produced in-river) is based on $IR_{SPM(sample)}$ = IR value of SPM sample in wet or dry season, IR_{soil} = IR value of nearest (upstream) O-soil, and $IR_{in\text{-}river}$ = end-member of in-river production (= 0.67). Following this model, the in-river produced fraction ranges from 0.06 to 1.0 and increases from the Madre de Dios headwaters to the lowlands in the wet season ($f_{in\text{-}river} = -0.2 *$ elevation (km) + 0.77, $R^2 = 0.73$). During the dry season, the contribution of in situ produced brGDGTs is generally ≥0.77 except above 2,777 mean catchment elevation, where the contribution is ≤0.60. Note that the end-member may have a partial contribution of soil-derived material and thus represents a rough estimate of in-river production. Since a robust data set of IR values generated by in situ production does not yet exist, the aquatic end-member may be specific for the Madre de Dios River. Further, it is not possible to differentiate between in-river produced and riverbank/floodplain-derived inputs in the lowlands based on our data, as both have high IR values. This implies that the fraction in-river produced is likely overestimated, especially in the lowlands where active floodplain and riverbank exchange takes place.

Regardless, 6-methyl brGDGTs have been found to respond to changes in (soil) pH rather than temperature (De Jonge, Hopmans, et al., 2014; Yang et al., 2015), which is instead recorded by the 5-methyl brGDGTs (De Jonge, Hopmans, et al., 2014; Naafs et al., 2017). Recently, Dang et al. (2016) reported that 6-methyl brGDGTs in global soils did not affect MAT reconstructions when they occur at relatively low levels

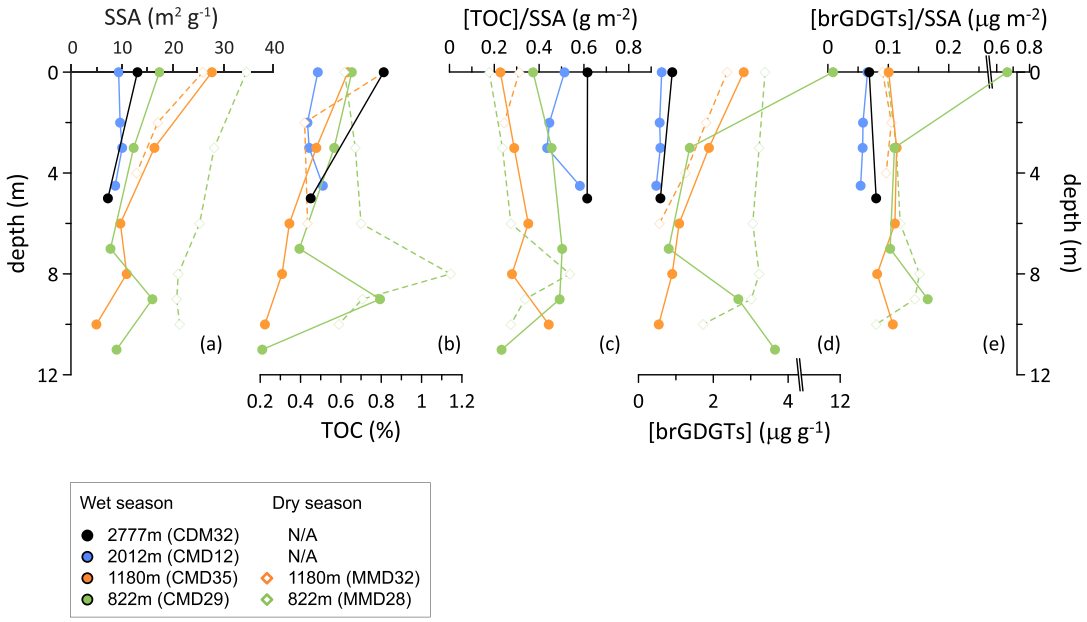

Figure 5. River depth profiles showing bulk properties of SPM during wet and dry seasons (a) SSA, (b) TOC, (c) [TOC]/SSA, (d) [brGDGTs], and (e) [brGDGTs]/SSA. Elevation is mean catchment elevation.

(IR < 0.5). Indeed, the clear temperature lapse rate for SPM in the Madre de Dios River suggests that the temperature signal is also unaffected by in-river production of 6-methyl brGDGTs.

3.6. BrGDGT Distributions Along River Depth Profiles

Previous studies have shown that suspended sediment transport by the Amazon River is influenced by hydrodynamic sorting (Bouchez et al., 2011; Guinoiseau et al., 2016), resulting in characteristic depth profiles, where the grain size of SPM increases toward the riverbed and SSA decreases (Figure 5a). This hydrodynamic sorting also influences OC profiles, as mineralogy and SSA often exert a control on the amount of OC transported as part of river SPM (Figures 5b and 5c; Bouchez et al., 2014). Feng et al. (2016) found that the Madre de Dios River has the expected grain size sorting within deep river channels and a "woody undercurrent" that transports high concentrations of relatively undegraded lignin above the sand layer. In contrast, plant wax *n*-alkanoic acids have been found to be well mixed based on their hydrogen isotopic composition (Ponton et al., 2014), although some sorting of the *n*-alkanes was noted based on their carbon isotopic composition (Feakins et al., 2018). The concentration of brGDGTs generally decreases with depth

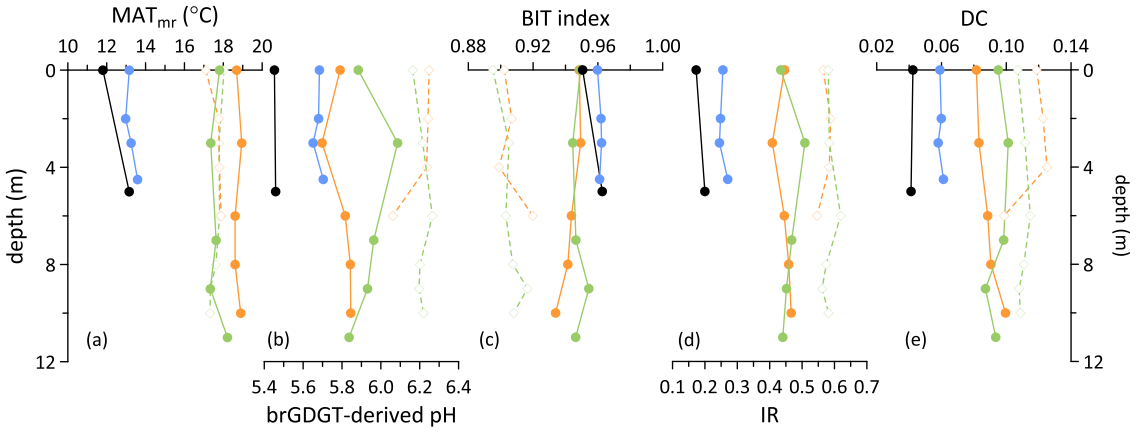

Figure 6. River depth profiles of brGDGT-based indices for SPM during wet and dry seasons (a) MAT_{mr}, (b) reconstructed pH, (c) BIT index, (d) IR, and (e) DC. Legend as in Figure 5.

(Figure 5d) but is constant when normalized to SSA (Figure 5e). Furthermore, all brGDGT-based indices are constant with depth at all sites, during both wet and dry seasons (Figure 6). This indicates that brGDGTs are generally very well mixed in the water column (following Peterse & Eglinton, 2017) and appear not sensitive to sorting. The only exception is station CMD-35 (1,180 m mean catchment elevation), where surface waters and the deepest sample contain very high concentrations of brGDGTs during the wet season (Figures 5d and 5e). However, the brGDGT-based proxies are invariable also at this station, indicating that there is no preferential transport of brGDGTs in the water column.

3.7. Connecting Headwaters to the Lower Amazon and River Fan

The concentration of brGDGTs in SPM in the Madre de Dios River (12–801 μg/g OC) is generally higher than that in the Lower Amazon River (13–230 μg/g OC near Óbidos; Zell, Kim, Abril, et al., 2013). This difference indicates that brGDGTs may be degraded during fluvial transport, or that they are diluted by aquatic primary production adding to the total OC pool in the lower part of the river. Indeed, annually and seasonally changing brGDGT concentrations and signatures in the Lower Amazon River were explained by variations in within-river production of brGDGTs related to varying hydrological conditions (Kim et al., 2012; Zell, Kim, Abril, et al., 2013). Although 5-methyl and 6-methyl brGDGT isomers were not separated and no IR values are available for Lower Amazon SPM, in situ production was recognized based on the higher DC of brGDGTs derived from recently living organisms and containing a polar headgroup opposed to that of "fossil" brGDGT core lipids without this headgroup in the river (Zell, Kim, Moreira-Turcq, et al., 2013). Furthermore, comparison of brGDGT signals in SPM from the Lower Amazon River with that in soils from the Andes (>2,500 m asl) and the lowlands (<500 m asl) showed that Lower Amazon SPM reflects a local, lowland soil signal that resembles (intermittently inundated) riverbank soils in particular (Zell, Kim, Moreira-Turcq, et al., 2013). .

While Andean erosion is considered to supply the majority of sediments to the lowland Amazon, lowland sources appear to become increasingly important for riverine OC and mineral composition of sediments, as changing OC signatures (Bouchez et al., 2014; Clark et al., 2017) and clay assemblages (Guyot et al., 2007) point toward active exchange with floodplains via bank erosion/deposition and flooding in the downstream Amazon basin. Similarly, brGDGT signatures in Madre de Dios River (this study) and Lower Amazon SPM (Kim et al., 2012; Zell, Kim, Abril, et al., 2013; Zell, Kim, Moreira-Turcq, et al., 2013) indicate that brGDGTs from the headwaters are replaced or overprinted by in situ production and/or local soil input upon reaching the lowlands. This supports the conceptual model proposed by Torres et al. (2017) wherein river-floodplain exchange drives the dilution ("shredding") of mountain-sourced biomarker signals downstream. In the modern Amazon basin, export of both OC and clastic material to the Atlantic Ocean is not directly coming from the Andes but seems to be a mixture of Andean material, bank/floodplain (re)mobilization, and in-river recycled OC and sediments. This has important implications for understanding the impact of river transport on OC cycling in the Amazon basin (e.g., Clark et al., 2017) and for the interpretation of biomarker signals in the sedimentary record (e.g., Bendle et al., 2010).

For instance, the historical development of the Amazon basin is much discussed. van Soelen et al. (2017) found that brGDGTs in Ceará Rise sediments in front of the Amazon River appear to have a terrestrial origin from the mid-Pliocene (4.5 Ma) to late-Pleistocene based on high fractional abundance of tetramethylated brGDGTs (%tetra; dominant (>90%) in modern soils and (>70%) in river SPM) combined with the low weighted number of cyclopentane moieties in the tetramethylated brGDGTs (#rings$_{tetra}$; dominant for in situ marine production, Sinninghe Damsté, 2016). However, a closer look reveals that this record is dominated by 6-methyl isomers and has IR values >0.6 (van Soelen et al., 2017). This implies that—although the source of this material is terrestrial—the majority of the brGDGTs originates from in-river production rather than soils. In addition, the low IR values for the Andean soils in the Madre de Dios River catchment (<0.2; Figure 3b) compared to those in the proximal sedimentary record at the Ceará Rise site indicate that a contribution of OC from the Andes is likely negligible. Interestingly, the Nd isotopic composition of the sediments at Ceará Rise implies that the mineral fraction is predominantly sourced from the Andes and thus suggests that during this period the transport of mineral and brGDGT fractions was decoupled. A further analysis of lacustrine sediments in floodplain lakes in the Lower Amazon River by Moreira et al. (2014) revealed that late Holocene brGDGT distributions differed from soils, which was attributed to in situ production. Specifically, high DC values were found and interpreted as resulting from fluvial input during high

river levels, suggesting close floodplain-river connectivity. This is in line with active phases of sediment aggregation on lowland floodplains over the Holocene, with sediments deposited and eroded in a meandering river system very similar to the modern-day river in the lower Madre de Dios catchment (Rigsby et al., 2009), implying a transient OC and sediment sink.

4. Conclusions

The brGDGTs in soils along an altitudinal transect in the Madre de Dios River basin record the adiabatic temperature trend of cooling with altitude in the Andean part of the transect; however, the proxy approximates saturation in the lowland sites. The brGDGTs are primarily transported during the wet season, when their signature in SPM reflects the same temperature gradient as in soils, albeit offset. This offset indicates that brGDGTs have an upland source relative to the catchment mean elevation, and that the initial Andean brGDGT signal is continuously modified by inputs from local soils during fluvial transit, evolving downstream. However, the loss of sensitivity of the proxy in lowland soils likely limits its use to similarly assess sourcing in the meandering part of the river, where the Andean soil-derived brGDGT signal becomes diluted by other sources.

A contribution of within-river produced and/or lowland floodplain/riverbank-derived brGDGTs can be recognized in the downstream deviation in the degrees of cyclization and isomerization of brGDGTs in SPM compared to in soils. The in situ produced brGDGTs seem to compose of primarily 6-methyl brGDGTs that are not sensitive to temperature and as such do not alter the temperature lapse rate based on 5-methyl brGDGTs in the SPM. Vertical sampling of depth profiles within deep sectors of the river (>6 m) during both wet and dry seasons shows that brGDGTs are not sorted by hydrodynamic processes, but that they are well mixed within the Madre de Dios River. The downstream accumulation of brGDGTs relative to TOC confirms their robustness as tracers for particulate soil OC in this tropical montane river.

While Andean erosion is assumed to supply the majority of clastic sediments to the downstream Amazon River, the increasing contribution of within river production of brGDGTs and continuous addition of local soil material downstream, in combination with the extensive lowland area in the Amazon basin (90% of catchment area), imply that the brGDGT signal finally discharged to the ocean is probably not influenced to a significant extent by Andean brGDGTs.

Acknowledgments
The brGDGT analyses were supported by NWO-Veni grant 863.13.016 to F.P. This material is based upon work supported by the US National Science Foundation under grant EAR-1227192 to A. J. W. and S. J. F. for the river fieldwork and lipid purification. In Perú, we thank the Servicio Nacional de Áreas Naturales Protegidas por el Estado (SERNANP) and personnel of Manu and Tambopata National Parks for logistical assistance and permission to work in the protected areas. We thank the Explorers' Inn and the Pontifical Catholic University of Perú (PUCP), as well as the Amazon Conservation Association for the use of the Tambopata and Wayqecha Research Stations, respectively. For river fieldwork assistance, we thank M. Torres, A. Robles, and A. Cachuana. Soil samples were contributed by Andrew Nottingham and Patrick Meir. Logistical support was provided by Y. Malhi, J. Huaman, W. Huaraca Huasco, and other collaborators as part of the Andes Biodiversity and Ecosystems Research Group ABERG (www.andesresearch.org). We thank Dominika Kasjaniuk for technical support at Utrecht. Two anonymous reviewers have provided valuable comments that have helped to improve this manuscript. Geochemical and brGDGT data are available in the PANGAEA Data Repository (Kirkels et al., 2019) and can be accessed at https://doi.pangaea.de/10.1594/PANGAEA.906170

References

AABP Atrium (Atrium Biodiversity Information System for the Andes to Amazon Biodiversity Program) of the Botanical Research Institute of Texas. http://atrium.andesamazon.org. Accessed 2018/06/20.

Asner, G. P., Anderson, C. B., Martin, R. E., Tupayachi, R., Knapp, D. E., & Sinca, F. (2015). Landscape biogeochemistry reflected in shifting distributionsof chemical traits in the Amazon forest canopy. *Nature Geoscience*, *8*, 567–573. https://doi.org/10.1038/NGEO2443

Aufdenkampe, A. K., Mayorga, E., Hedges, J. I., Llerena, C., Quay, P. D., Gudeman, J., et al. (2007). Organic matter in the Peruvian headwaters of the Amazon: Compositional evolution from the Andes to the lowland Amazon mainstem. *Frontiers in Ecology and the Environment*, *38*(3), 337–364. https://doi.org/10.1016/j.orggeochem.2006.06.003

Bendle, J. A., Weijers, J. W. H., Maslin, M. A., Sinninghe Damsté, J. S., Schouten, S., Hopmans, E. C., et al. (2010). Major changes in glacial and Holocene terrestrial temperatures and sources of organic carbon recorded in the Amazon fan by tetraether lipids. *Geochemistry, Geophysics, Geosystems*, *11*, Q12007. https://doi.org/10.1029/2010GC003308

Berner, R. A. (1982). Burial of organic carbon and pyrite sulfur in the modern ocean; its geochemical and environmental significance. *American Journal of Science*, *282*, 451–473. https://doi.org/10.2475/ajs.282.4.451

Bianchi, T. S., Wysocki, L. A., Stewart, M., Filley, T. R., & McKee, B. A. (2007). Temporal variability in terrestrially-derived sources of particulate organic carbon in the lower Mississippi River and its upper tributaries. *Geochimica et Cosmochimica Acta*, *71*, 4425–4437. https://doi.org/10.1016/j.gca.2007.07.011

Blair, N. E., & Aller, R. C. (2012). The fate of terrestrial organic carbon in the marine environment. *Annual Review of Marine Science*, *4*(1), 401–423. https://doi.org/10.1146/annurev-marine-120709-142717

Bouchez, J., Gaillardet, J., France-Lanord, C., Laurence, M., & Dutra-Maia, P. (2011). Grain size control of river suspended sediment geochemistry: Clues from Amazon River depth profiles. *Geochemistry, Geophysics, Geosystems*, *12*, Q03008. https://doi.org/10.1029/2010GC003380

Bouchez, J., Galy, V., Hilton, R. G., Gaillardet, J., Moreira-Turcq, P., Pérez, M. A., et al. (2014). Source, transport and fluxes of Amazon River particulate organic carbon: Insights from river sediment depth-profiles. *Geochimica et Cosmochimica Acta*, *133*, 280–298. https://doi.org/10.1016/j.gca.2014.02.032

Cai, D. -L., Tan, F. C., & Edmond, J. M. (1988). Sources and transport of particulate organic carbon in the Amazon River and estuary. *Estuarine, Coastal and Shelf Science*, *26*, 1–14. https://doi.org/10.1016/0272-7714(88)90008-X

Chadwick, K. D., & Asner, G. P. (2016). Tropical soil nutrient distributions determined by biotic and hillslope processes. *Biogeochemistry*, *127*(2-3), 273–289. https://doi.org/10.1007/s10533-015-0179-z

Clark, K. E., Hilton, R. G., West, A. J., Robles Caceres, A., Gröcke, D. R., Marthews, T. R., et al. (2017). Erosion of organic carbon from the Andes and its effects on ecosystem carbon dioxide balance. *Journal of Geophysical Research: Biogeosciences*, *122*, 449–469. https://doi.org/10.1002/2016JG003615

Clark, K. E., West, A. J., Hilton, R. G., Asner, G. P., Quesada, C. A., Silman, M. R., et al. (2016). Storm-triggered landslides in the Peruvian Andes and implications for topography, carbon cycles, and biodiversity. *Earth Surface Dynamics*, *4*(1), 47–70. https://doi.org/10.5194/esurf-4-47-2016

Coffinet, S., Huguet, A., Pedentchouk, N., Bergonzini, L., Omuombo, C., Williamson, D., et al. (2017). Evaluation of branched GDGTs and leaf wax n-alkane δ2H as (paleo) environmental proxies in East Africa. *Geochimica et Cosmochimica Acta*, *198*, 182–193. https://doi.org/10.1016/j.gca.2016.11.020

Dang, X., Yang, H., Naafs, B. D. A., Pancost, R. D., & Xie, S. (2016). Evidence of moisture control on the methylation of branched glicerol dialkyl glicerol tetraethers in semi-arid and arid soils. *Geochimica et Cosmochimica Acta*, *198*, 24–36. https://doi.org/10.1016/j.gca.2016.06.004

De Jonge, C., Hopmans, E. C., Zell, C. I., Kim, J. -H., Schouten, S., & Sinninghe Damsté, J. S. (2014). Occurrence and abundance of 6-methyl branched glycerol dialkyl glycerol tetraethers in soils: Implications for palaeoclimate reconstruction. *Geochimica et Cosmochimica Acta*, *141*, 97–112. https://doi.org/10.1016/j.gca.2014.06.013

De Jonge, C., Stadnitskaia, A., Hopmans, E. C., Cherkashov, G., Fedotov, A., & Sinninghe Damsté, J. S. (2014). In situ produced branched glycerol dialkyl glycerol tetraethers in suspended particulate matter from the Yenisei River, Eastern Siberia. *Geochimica et Cosmochimica Acta*, *125*, 476–491. https://doi.org/10.1016/j.gca.2013.10.031

Deng, L., Jia, G., Jin, C., & Shijie, L. (2016). Warm season bias of branched GDGT temperature estimates causes underestimation of altitudinal lapse rate. *Organic Geochemistry*, *96*, 11–17. https://doi.org/10.1016/j.orggeochem.2016.03.004

Ernst, N., Peterse, F., Breitenbach, S. F. M., Syiemlieh, H. J., & Eglinton, T. I. (2013). Biomarkers record environmental changes along an altitudinal transect in the wettest place on Earth. *Organic Geochemistry*, *60*, 93–99. https://doi.org/10.1016/j.orggeochem.2013.05.004

Espinoza, J. C., Steven, C., Josyane, R., Clémentine, J., Ken, T., & Waldo, L. (2015). Rainfall hotspots over the southern tropical Andes: Spatial distribution, rainfall intensity, and relations with large-scale atmospheric circulation. *Water Resources Research*, *51*, 3459–3475. https://doi.org/10.1002/2014WR016273

Eva, H. D., & Huber, O. (2005). *A proposal for defining the geographical boundaries of Amazonia; Synthesis of the results of an expert consultation workshop organized by the European Commission in collaboration with the Amazon Cooperation Treaty Organization*. Luxembourg: Office for Official Publications of the European Communities.

Feakins, S. J., Wu, M. S., Ponton, C., Galy, V., & West, A. J. (2018). Dual isotope evidence for sedimentary integration of plant wax biomarkers across an Andes-Amazon elevation transect. *Geochimica et Cosmochimica Acta*, *242*, 64–81. https://doi.org/10.1016/j.gca.2018.09.007

Feng, X., Feakins, S. J., Liu, Z., Ponton, C., Wang, R. Z., Karkabi, E., et al. (2016). Source to sink: Evolution of lignin composition in the Madre de Dios River system with connection to the Amazon basin and offshore. *Journal of Geophysical Research: Biogeosciences*, *121*, 1316–1338. https://doi.org/10.1002/2016JG003323

France-Lanord, C., & Derry, L. A. (1994). $\delta^{13}C$ of organic carbon in the Bengal Fan: Source evolution and transport of C3 and C4 plant carbon to marine sediments. *Geochimica et Cosmochimica Acta*, *58*, 4809–4814.

Freymond, C. V., Kündig, N., Stark, C., Peterse, F., Buggle, B., Lupker, M., et al. (2018). Evolution of biomolecular loadings along a major river system. *Geochimica et Cosmochimica Acta*, *223*, 389–404. https://doi.org/10.1016/j.gca.2017.12.010

Freymond, C. V., Peterse, F., Fischer, L. V., Filip, F., Giosan, L., & Eglinton, T. I. (2017). Branched GDGT signals in fluvial sediments of the Danube River basin: Method comparison and longitudinal evolution. *Organic Geochemistry*, *107*, 88–96. https://doi.org/10.1016/j.orggeochem.2016.11.002

Galy, V., France-Lanord, C., Beyssac, O., Faure, P., Kudrass, H., & Palhol, F. (2007). Efficient organic carbon burial in the Bengal fan sustained by the Himalayan erosional system. *Nature*, *450*, 407–410. https://doi.org/10.1038/nature06273

Galy, V., France-Lanord, C., & Lartiges, B. (2008). Loading and fate of particulate organic carbon from the Himalaya to the Ganga–Brahmaputra delta. *Geochimica et Cosmochimica Acta*, *72*, 1767–1787. https://doi.org/10.1016/j.gca.2008.01.027

Girardin, C. A. J., Espejob, J. E. S., Doughty, C. E., Huasco, W. H., Metcalfe, D. B., Durand-Baca, L., et al. (2014). Productivity and carbon allocation in a tropical montane cloud forest in the Peruvian Andes. *Plant Ecology and Diversity*, *7*(1-2), 107–123. https://doi.org/10.1080/17550874.2013.820222

Goñi, M. A., Ruttenberg, K. C., & Eglinton, T. I. (1997). Sources and contribution of terrigenous organic carbon to surface sediments in the Gulf of Mexico. *Nature*, *389*, 275–278. https://doi.org/10.1038/38477

Guinoiseau, D., Bouchez, J., Gélabert, A., Louvat, P., Filizola, N., & Benedetti, M. F. (2016). The geochemical filter of large river confluences. *Chemical Geology*, *441*, 191–203. https://doi.org/10.1016/j.chemgeo.2016.08.009

Guyot, J. L., Jouanneau, J. M., Soares, L., Boaventura, G. R., Maillet, N., & Lagane, C. (2007). Clay mineral composition of river sediments in the Amazon Basin. *Catena*, *71*, 340–356. https://doi.org/10.1016/j.catena.2007.02.002

Guyot, J. L., & Wasson, J. G. (1994). Regional pattern of riverine dissolver organic carbon in the Amazon drainage basin of Bolivia. *Limnology and Oceanography*, *39*, 452–458.

Hamilton, S. K., Kellndorfer, J., Lehner, B., & Tobler, M. (2007). Remote sensing of floodplain geomorphology as a surrogate for biodiversity in a tropical river system (Madre de Dios, Peru). *Geomorphology*, *89*, 23–38. https://doi.org/10.1016/j.geomorph.2006.07.024

Hedges, J. I., Mayorga, E., Tsamakis, E., McClain, M. E., Aufdenkampe, A., Quay, P., et al. (2000). Organic matter in Bolivian tributaries of the Amazon River: A comparison to the lower mainstream. *Limnology and Oceanography*, *45*(7), 1449–1466. https://doi.org/10.4319/lo.2000.45.7.1449

Hemingway, J. D., Schefuß, E., Spencer, R. G. M., Dinga, B. J., Eglinton, T. I., McIntyre, C., & Galy, V. V. (2017). Hydrologic controls on seasonal and inter-annual variability of Congo River particulate organic matter source and reservoir age. *Chemical Geology*, *466*, 454–465. https://doi.org/10.1016/j.chemgeo.2017.06.034

Hoorn, C., Wesselingh, F. P., ter Steege, H., Bermudez, M. A., Mora, A., Sevink, J., et al. (2010). Amazonia through time: Andean uplift, climate change, landscape evolution, and biodiversity. *Science*, *330*(6006), 927–931. https://doi.org/10.1126/science.1194585

Hopmans, E. C., Schouten, S., & Sinninghe Damsté, J. S. (2016). The effect of improved chromatography on GDGT-based palaeoproxies. *Organic Geochemistry*, *93*, 1–6. https://doi.org/10.1016/j.orggeochem.2015.12.006

Hopmans, E. C., Weijers, J. W. H., Schefuß, E., Herfort, L., Sinninghe Damsté, J. S., & Schouten, S. (2004). A novel proxy for terrestrial organic matter in sediments based on branched and isoprenoid tetraether lipids. *Earth and Planetary Science Letters*, *224*(1-2), 107–116. https://doi.org/10.1016/j.epsl.2004.05.012

Householder, J. E., Janovec, J. P., Tobler, M. T., Page, S., & Lähteenoja, O. (2012). Peatlands of the Madre de Dios River of Peru: Distribution, geomorphology, and habitat diversity. *Wetlands*, *32*, 359–368. https://doi.org/10.1007/s13157-012-0271-2

Huasco, W. H., Girardin, C. A. J., Doughty, C. E., Metcalfe, D. B., Baca, L. D., Silva-Espejo, J. E., et al. (2014). Seasonal production, allocation and cycling of carbon in two mid-elevation tropical montane forest plots in the Peruvian Andes. *Plant Ecology and Diversity*, *7*(1-2), 125–142. https://doi.org/10.1080/17550874.2013.819042

Huguet, C., Hopmans, E. C., Febo-Ayala, W., Thompson, D. H., Sinninghe Damsté, J. S., & Schouten, S. (2006). An improved method to determine the absolute abundance of glycerol dibiphytanyl glycerol tetraether lipids. *Organic Geochemistry*, *37*(9), 1036–1041. https://doi.org/10.1016/j.orggeochem.2006.05.008

Keil, R. G., Mayer, L. M., Quay, P. D., Richey, J. E., & Hedges, J. I. (1997). Loss of organic matter from riverine particles in deltas. *Geochimica et Cosmochimica Acta*, *61*, 1507–1511. https://doi.org/10.1016/S0016-7037(97)00044-6

Killeen, T. J., Michael, D., Trisha, C., Jørgensen, P. M., & John, M. (2007). Dry spots and wet spots in the Andean hotspot. *Journal of Biogeography*, *34*(8), 1357–1373. https://doi.org/10.1111/j.1365-2699.2006.01682.x

Kim, J. -H., Zell, C., Moreira-Turcq, P., Pérez, M. A. P., Abril, G., Mortillaro, J. -M., et al. (2012). Tracing soil organic carbon in the lower Amazon River and its tributaries using GDGT distributions and bulk organic matter properties. *Geochimica et Cosmochimica Acta*, *90*, 163–180. https://doi.org/10.1016/j.gca.2012.05.014

Kirkels, F., Ponton, C., Galy, V., West, A. J., Feakins, S. J, & Peterse, F. (2019). Analysis of brGDGTs as tracers for soil organic carbon in the Madre de Dios River system. PANGAEA. https://doi.org/10.1594/PANGAEA.906170

Lei, Y., Yang, H., Dang, X., Zhao, S., & Xie, S. (2016). Absence of a significant bias towards summer temperature in branched tetraether-based paleothermometer at two soil sites with contrasting temperature seasonality. *Organic Geochemistry*, *94*, 83–94. https://doi.org/10.1016/j.orggeochem.2016.02.003

Malhi, Y., Farfán Amézquita, F., Doughty, C. E., Silva-Espejo, J., Girardin, C., Metcalfe, D. B., & Phillips, O. L. (2014). The productivity, metabolism and carbon cycle of two lowland tropical forest plots in south-western Amazonia, Peru. *Plant Ecology and Diversity*, *7*(1-2), 85–105. https://doi.org/10.1080/17550874.2013.820805

Marengo, J. A., Soares, W. R., Saulo, C., & Nicolini, M. (2004). Climatology of the low-level jet east of the Andes as derived from the NCEP–NCAR reanalyses: Characteristics and temporal variability. *Journal of Climate*, *17*(12), 2261–2280. https://doi.org/10.1175/1520-0442(2004)0172.0.CO;2

Mayer, L. M. (1994). Surface area control of organic carbon accumulation in continental shelf sediments. *Geochimica et Cosmochimica Acta*, *58*, 1271–1284. https://doi.org/10.1016/0016-7037(94)90381-6

Mayorga, E., Aufdenkampe, A. K., Masiello, C. A., Krusche, A. V., Hedges, J. I., Quay, P. D., et al. (2005). Young organic matter as a source of carbon dioxide outgassing from Amazonian rivers. *Nature*, *436*(7050), 538–541. https://doi.org/10.1038/nature03880

McClain, M. E., & Naiman, R. J. (2008). Andean influences on the biogeochemistry and ecology of the Amazon River. *Bioscience*, *58*(4), 325–338. https://doi.org/10.1641/B580408

Meade, R. H., Dunne, T., Richey, J. E., Santos, U. D. M., & Salati, E. (1985). Storage and remobilization of suspended sediment in the lower Amazon River of Brazil. *Science*, *228*(4698), 488–490. https://doi.org/10.1126/science.228.4698.488

Moreira, L. S., Moreira-Turcq, P., Kim, J. H., Turcq, B., Cordeiro, R. C., Mandengo-Yogo, M., & Sinninghe-Damsté, J. S. (2014). A mineralogical and organic geochemical overview of the effects of Holocene changes in Amazon River flow on three floodplain lakes. *Paleogeography, Paleoclimatology, Paleoecology*, *415*, 152–164. https://doi.org/10.1016/j.palaeo.2014.03.017

Naafs, B. D. A., Gallego-Sala, A. V., Inglis, G. N., & Pancost, R. D. (2017). Refining the global branched glycerol dialkyl glycerol tetraether (brGDGT) soil temperature calibration. *Organic Geochemistry*, *106*, 48–56. https://doi.org/10.1016/j.orggeochem.2017.01.009

Nieto-Moreno, V., Rohrmann, A., van der Meer, M. T. J., Sinninghe Damsté, J. S., Sachse, D., Tofelde, S., et al. (2016). Elevation-dependent changes in n-alkane δD and soil GDGTs across the south central Andes. *Earth and Planetary Science Letters*, *453*, 234–242. https://doi.org/10.1016/j.epsl.2016.07.049

Nottingham, A. T., Turner, B. L., Whitaker, J., Ostle, N. J., McNamara, N. P., Bardgett, R. D., et al. (2015). Soil microbial nutrient constraints along a tropical forest elevation gradient: A belowground test of a biogeochemical paradigm. *Biogeosciences*, *12*(20), 6071–6083. https://doi.org/10.5194/bg-12-6071-2015

Nottingham, A. T., Whitaker, J., Turner, B. L., Salinas, N., Zimmermann, M., Malhi, Y., & Meir, P. (2015). Climate warming and soil carbon in tropical forests: Insights from an elevation gradient in the Peruvian Andes. *Bioscience*, *65*(9), 906–921. https://doi.org/10.1093/biosci/biv109

Onstad, G. D., Canfield, D. E., Quay, P. D., & Hedges, J. I. (2000). Sources of particulate organic matter in rivers from the continental USA: Lignin phenol and stable carbon isotope compositions. *Geochimica et Cosmochimica Acta*, *64*, 3539–3546. https://doi.org/10.1016/S0016-7037(00)00451-8

Osher, L. J., & Buol, S. W. (1998). Relationships of soil properties to parent material and landscape position in eastern Madre de Dios, Peru. *Geoderma*, *83*, 143–166.

Peterse, F., & Eglinton, T. I. (2017). Grain size associations of branched tetraether lipids in soils and riverbank sediments: Influence of hydrodynamic sorting processes. *Frontiers in Earth Science*, *5*, 49. https://doi.org/10.3389/feart.2017.00049

Ponton, C., West, J. A., Feakins, S. J., & Galy, V. (2014). Leaf wax biomarkers in transit record river catchment composition. *Geophysical Research Letters*, *41*, 6420–6427. https://doi.org/10.1002/2014GL061328

Prahl, F. G., Ertel, J. R., Goni, M. A., Sparrow, M. A., & Eversmeyer, B. (1994). Terrestrial organic carbon contributions to sediments on the Washington margin. *Geochimica et Cosmochimica Acta*, *58*, 3035–3048. https://doi.org/10.1016/0016-7037(94)90177-5

Quesada, C. A., Lloyd, J., Schwarz, M., Patiño, S., Baker, T. R., Czimczik, C., et al. (2010). Variations in chemical and physical properties of Amazon forest soils in relation to their genesis. *Biogeosciences*, *7*(5), 1515–1541. https://doi.org/10.5194/bg-7-1515-2010

Rapp, J. M., & Silman, M. R. (2012). Diurnal, seasonal, and altitudinal trends in microclimate across a tropical montane cloud forest. *Climate Research*, *55*(1), 17–32. https://doi.org/10.3354/cr01127

Rigsby, C. A., Hemric, E. M., & Baker, P. (2009). Later Quaternary paleohydrology of the Madre de Dios River, southwestern Amazon Basin, Peru. *Geomorphology*, *113*, 158–172. https://doi.org/10.1016/j.geomorph.2008.11.017

Sinninghe Damsté, J. J., Ossebaar, J., Abbas, B., Schouten, S., & Verschuren, D. (2009). Fluxes and distribution of tetraether lipids in an equatorial African lake: Constraints on the application of the TEX_{86} palaeothermometer and BIT index in lacustrine settings. *Geochimica et Cosmochimica Acta*, *73*, 4232–4249. https://doi.org/10.1016/j.gca.2009.04.022

Sinninghe Damsté, J. S. (2016). Spatial heterogeneity of sources of branched tetraethers in shelf systems: The geochemistry of tetraethers in the Berau River delta (Kalimantan, Indonesia). *Geochimica et Cosmochimica Acta*, *186*, 13–31. https://doi.org/10.1016/j.gca.2016.04.033

Sinninghe Damsté, J. S., Ossebaar, J., Schouten, S., & Verschuren, D. (2008). Altitudinal shifts in the branched tetraether lipid distribution in soil from Mt. Kilimanjaro (Tanzania): Implications for the MBT/CBT continental palaeothermometer. *Organic Geochemistry*, *39*, 1072–1076. https://doi.org/10.1016/j.orggeochem.2007.11.011

Torres, M. A., Limaye, A. B., Ganti, V., Lamb, M. P., West, A. J., & Fischer, W. W. (2017). Model predictions of long-lived storage of organic carbon in river deposits. *Earth Surface Dynamics*, *5*, 711–730. https://doi.org/10.5194/esurf-5-711-2017

Townsend-Small, A., McClain, M. E., & Brandes, J. A. (2005). Contributions of carbon and nitrogen from the Andes Mountains to the Amazon River: Evidence from an elevational gradient of soils, plants, and river material. *Limnology and Oceanography*, *50*, 672–685.

Townsend-Small, A., McClain, M. E., Hall, B., Noguera, J. L., Llerena, C. A., & Brandes, J. A. (2008). Suspended sediments and organic matter in mountain headwaters of the Amazon River: Results from a 1-year time series study in the central Peruvian Andes. *Geochimica et Cosmochimica Acta*, *72*, 732–740. https://doi.org/10.1016/j.gca.2007.11.020

van Soelen, E. E., Kim, J. H., Santos, R. V., Dantas, E. L., Vasconcelos de Almeida, F., Pires, J. P., et al. (2017). A 30 Ma history of the Amazon River inferred from terrigenous sediments and organic matter on the Ceará Rise. *Earth and Planetary Science Letters*, *474*, 40–48. https://doi.org/10.1016/j.epsl.2017.06.025

Weijers, J. W. H., Bernhardt, B., Peterse, F., Werne, J. P., Dungait, J. A. J., Schouten, S., & Sinninghe Damsté, J. S. (2011). Absence of seasonal patterns in MBT–CBT indices in mid-latitude soils. *Geochimica et Cosmochimica Acta*, *75*, 3179–3190. https://doi.org/10.1016/j.gca.2011.03.015

Weijers, J. W. H., Schefuß, E., Schouten, S., & Sinninghe Damsté, J. S. (2007). Coupled thermal and hydrological evolution of tropical Africa over the last deglaciation. *Science*, *315*(5819), 1701–1704. https://doi.org/10.1126/science.1138131

Weijers, J. W. H., Schouten, S., Spaargaren, O. C., & Sinninghe Damsté, J. S. (2006). Occurrence and distribution of tetraether membrane lipids in soils: Implications for the use of the TEX_{86} proxy and the BIT index. *Organic Geochemistry*, *37*(12), 1680–1693. https://doi.org/10.1016/j.orggeochem.2006.07.018

Weijers, J. W. H., Schouten, S., van den Donker, J. C., Hopmans, E. C., & Sinninghe Damsté, J. S. (2007). Environmental controls on bacterial tetraether membrane lipid distribution in soils. *Geochimica et Cosmochimica Acta*, *71*(3), 703–713. https://doi.org/10.1016/j.gca.2006.10.003

Wissmar, R. C., Richey, J. E., Stallard, R. F., & Edmond, J. M. (1981). Plankton metabolism and carbon processes in the Amazon River, its tributaries, and floodplain waters, Peru-Brazil, May-June 1977. *Ecology*, *62*, 1622–1633.

Yang, H., Lü, X., Ding, W., Lei, Y., Dang, X., & Xie, S. (2015). The 6-methyl branched tetraethers significantly affect the performance of the methylation index (MBT0) in soils from an altitudinal transect at Mount Shennongjia. *Organic Geochemistry*, *82*, 42–53. https://doi.org/10.1016/j.orggeochem.2015.02.003

Zang, J., Lei, Y., & Yang, H. (2018). Distribution of glycerol ethers in Turpan soils: Implications for use of GDGT-based proxies in hot and dry regions. *Frontiers of Earth Science*, *12*(4), 862–876. https://doi.org/10.1007/s11707-018-0722-z

Zell, C., Kim, J., Abril, G., Sobrinho, R., Dorhout, D., Moreira-Turcq, P., & Sinninghe Damsté, J. (2013). Impact of seasonal hydrological variation on the distributions of tetraether lipids along the Amazon River in the central Amazon basin: Implications for the MBT/CBT paleothermometer and the BIT index. *Frontiers in Microbiology*, *4*, 228. https://doi.org/10.3389/fmicb.2013.00228

Zell, C., Kim, J. H., Moreira-Turcq, P., Abril, G., Hopmans, E. C., Bonnet, M. P., et al. (2013). Disentangling the origins of branched tetraether lipids and crenarchaeol in the lower Amazon River: Implications for GDGT-based proxies. *Limnology and Oceanography*, *58*(1), 343–353. https://doi.org/10.4319/lo.2013.58.1.0343

Zhu, C., Weijers, J. W. H., Wagner, T., Pan, J. -M., Chen, J. -F., & Pancost, R. D. (2011). Sources and distributions of tetraether lipids in surface sediments across a large river-dominated continental margin. *Organic Geochemistry*, *42*(4), 376–386. https://doi.org/10.1016/j.orggeochem.2011.02.002

Zimmermann, M., Leifeld, J., Conen, F., Bird, M. I., & Meir, P. (2010). Can composition and physical protection of soil organic matter explain soil respiration temperature sensitivity? *Biogeochemistry*, *107*(1-3), 423–436. https://doi.org/10.1007/s10533-010-9562-y

Zimmermann, M., Meir, P., Bird, M., Mahli, Y., & Ccahuana, A. (2009). Climate dependence of heterotrophic soil respiration from a soil-translocation experiment along a 3000 m tropical forest altitudinal gradient. *European Journal of Soil Science*, *60*, 895–906. https://doi.org/10.1111/j.1365-2389.2009.01175.x

Zimmermann, M., Meir, P., Bird, M. I., Malhi, Y., & Ccahuana, A. J. (2010). Temporal variation and climate dependence of soil respiration and its components along a 3000 m altitudinal tropical forest gradient. *Global Biogeochemical Cycles*, *24*, GB4012. https://doi.org/10.1029/2010GB003787